Supporting information for *CrystEngComm*. 2022

Ultrasensitive fluorescence detection of norfloxacin in aqueous medium employment a 2D Zn(II)-based coordination polymer

Na-Na Zeng[b], Li Ren [a,]*, Guang-Hua Cui[b,]*

a Qian'an College, North China University of Science and Technology, Qian'an, Tangshan, Hebei, 064400, P. R. China

b College of Chemical Engineering, Hebei Key Laboratory for Environment Photocatalytic and Electrocatalytic Materials, North China University of Science and Technology, No. 21 Bohai Road, Caofeidian new-city, Tangshan, Hebei, 063210, P. R. China

Corresponding author: Li-Ren; Guang-Hua Cui

Fax: +86–0315–8805462. Tel: +86–0315–8805460.

E-mail: renlilsj420@163.com*;* tscghua@126.com

CONTENTS

Section 1. Experimental Section

1. Materials and methods
2. Preparation of {[$Zn(L)_{0.5}$(mip)] $1.75H_2O$}n (**1**)
3. X-ray crystallography
4. The fluorescence lifetime
5. Stabilities
6. Fluorescence detection of antibiotics in water
7. The performance of regeneration
8. Electrochemical measurements
9. References

1. Materials and methods

The L ligand was prepared according to the previously reported method [1]. All other chemicals of reagent grade were commercially available and used without further purification. Elemental analyses of C, H, and N were carried out on a Perkin-Elmer 240C elemental analyzer. The powder X-ray diffraction (PXRD) tests were measured on a Rigaku D/Max-2500PC diffractometer (λ = 1.5418 Å) at room temperature. The IR spectra were collected within the 4000–400 cm^{-1} region on a Bruker VERTEX 80V FT-IR spectrophotometer. The thermogravimetric analysis (TGA) was recorded using a Netzsch STA449 F1 thermal analyzer under an air atmosphere while the heating rate was ramped from room temperature to 800 °C at 10 °C/min. Fluorescence spectra and luminescence lifetime were monitored using an Edinburgh FS5 spectrograph. The UV-Vis diffuse reflectance spectra (DRS), as well as the absorption spectra, were recorded on a Persee T9 ultraviolet-visible spectrometer at ambient temperature. The CHI660E electrochemical workstation with a three-electrode system was used for electrochemical measurements.

2. Preparation of {[$Zn(L)_{0.5}$(mip)] $1.75H_2O$}n (1)

1 was prepared by mixed $Zn(OAc)_2 \cdot 2H_2O$ (0.20 mmol, 43.9 mg), H_2mip (0.20 mmol, 35.6 mg), L ligand (0.05 mmol, 25.2 mg) and 10 mL of distilled water. The solution was transformed into a 25 mL Teflon-lined stainless-steel reactor, sealed, heated to 140 ℃ for 72 h. Then after the mixture was cooled to ambient temperature, colorless block transparent crystals were obtained with 43.2% yield based on the L ligand. Elemental analysis for $C_{92}H_{78}N_{12}O_{23}S_4Zn_4$ (Mr = 2109.45): C, 52.38%; H, 3.73%; N, 7.97%. Found: C, 52.63%; H, 3.57%, N, 7.78%. IR: 3436(s), 2923(w), 1624(m), 1403(w), 1367(w), 1303(w), 910(m) and 742(w) (Fig. S1).

3. X-ray crystallography

The diffraction data of the single crystal **1** were collected at 293(2) K by a Bruker Smart CCD diffractometer (Mo–Kα radiation, λ = 0.71073 Å, ω–φ scan) [2]. The absorption corrections were applied using the multi-scan program *via* SADABS [3]. The structure was solved by the direct method (SHELXT-2015) and refined through full-matrix least-squares on F^2 (SHELXL-2018) in the anisotropic approximation (except hydrogen atoms) [4]. The positions of hydrogen atoms of the organic ligands were calculated geometrically and refined in the riding model. And the hydrogen atoms of the water molecules were located from difference maps and refined with isotropic temperature factors. The detailed crystallographic data and structure refinement parameters for **1** are served in Table S1, the selected bond distances and angles for the title CP are summarized in Table S2.

4. The fluorescence lifetime

The fluorescence decay curve of **1** was recorded by an FS5 fluorescence spectrometer with a F^2 microsecond flashlamp light source. The fluorescence lifetime (τ) of the strongest emission peak (370 nm) and excitation peak (304 nm) was measured and fitted by a double-exponential model [5]:

$$R(\tau) = \frac{B_1\tau_1^2 + B_2\tau_2^2}{B_1\tau_1 + B_2\tau_2}$$

5. Stabilities

The thermal stability of **1** was studied by thermogravimetric analysis (TGA). In addition, chemical stability should also be considered in practical applications. Powders **1** were immersed in acidic and alkaline aqueous solutions (pH = 1−14) at room temperature and the emission spectra were recorded.

6. Fluorescence detection of antibiotics in water

The fluorescence of **1** in various solvents was measured on the spectrophotometer equipped with a 1×1 cm^2 quartz cell. To evaluate selectivity and sensitivity of **1** to some common antibiotics, including ENR (enrofloxacin), SDZ (sulfadiazine), SMZ (sulfamethazine), SMX (sulfamethoxazole), ORN (ornidazole), RNZ (ronidazole), LEV (levofloxacin), NOR (norfloxacin), CIP (ciprofloxacin), MDZ (metronidazole), 1×10^{-4} mol/L antibiotic solutions were prepared *via* dissolving a certain amount of antibiotics in deionized water or organic solvents. Then, ground powder of **1** (4 mg) was dissolved in 4 mL above antibiotic solutions, respectively, and ultrasonically stirred for 30 min to obtain stable suspension solutions for fluorescence sensing experiments. To check the sensing ability of **1** towards different antibiotics, fluorescence titration spectra were performed by gradually adding 10^{-3} mol/L stock solutions of the above ten antibiotics.

The fluorescent quenching effect of NOR was quantitatively interpreted by fitting the experimental data with the Stern-Volmer (S-V) equation: $I/I_0 = 1 + K_{sv}$ [M], I_0 is the initial fluorescence intensity without antibiotic, I represents the fluorescence intensity with the added antibiotic of the molar concentration [M], and K_{sv} is the S-V constant (L/mol) that directly represents the sensitivity of fluorescence quenching, respectively [6].

7. The performance of regeneration

The regeneration or reusability of a sensory material is also important in practical application. To better analyze the recyclability of **1**, the cyclic experiment was carried out. Sample **1** was recovered by centrifuging, washing with distilled water (5 mL × 2) and alcohol (5 mL × 2) successively, and drying at 60 ℃ for 2 h after it was used in a fluorescence quenching experiment for the analyte, and the regenerated sample was used again for the experiment.

8. Electrochemical measurements

Using the 0.2 mol/L Na_2SO_4 aqueous solution as the electrolyte, the reference and counter electrodes were Ag/AgCl and platinum wire, respectively. The work electrodes were prepared according to the following steps: First, clean the FTO conductive glass substrates in ethanol and distilled water successively. Then, disperse 5 mg of sample powders into 20 μL of 0.2% Nafion solution to obtain slurries. Finally, drop the prepared slurries onto an FTO slice with an effective working area of 1 cm^2 and dry it at 60 °C for 2 h. Mott-Schottky plots were collected on a BioLogic VSP-300 electrochemical system with a 30 W Xenon lamp irradiation to obtain the intrinsic features of the flat-band potentials at the frequencies of 1500, 2000, and 2500 Hz [7].

References

[1] R. Bronisz. *Inorg. Chem.*, 2015, **44**, 4463.

[2] X. M. Kang, X. Y. Fan and P. Y. Hao, *Inorg. Chem. Front.*, 2019, **6**, 271.

[3] G. Ji, J. Liu and X. Gao, *J. Mater. Chem. A*, 2017, **5**, 10200.

[4] G. M. Sheldrick, *Struct. Chem.*, 2015, **71**, 3.

[5] X. Liu, Q. Ma, X. Feng, R. Li and X. Zhang, *Microchem. J.,* 2021, **170**, 106714.

[6] D. Wang, J. Wang, M. Daniel, C. B. Guillermo and J. H. Alan, *Langmuir*, 2001, **17**, 1262.

[7] X. J. Wen, C. G. Niu, L. Zhang and G. M. Zeng, *ACS Sustain. Chem. Eng.*, 2017, **5**, 5134.

Section 2. Supplementary Tables

Table S1. Crystal and refinement data for **1**

Table S2. The selected bond lengths (Å) and angles (°) for **1**

Table S3. Comparison of analytical methods for the detecting NOR

Table S4. The HOMO-LUMO energies calculated for selected analytes

Table S1. Crystal and refinement data for **1**

	1
Empirical formula	$C_{92}H_{78}N_{12}O_{23}S_4Zn_4$
Formula weight	2109.38
Crystal system	monoclinic
Space group	$P2_1/n$
a (Å)	8.892(4)
b (Å)	24.276(11)
c (Å)	11.365(5)
α (°)	90
β (°)	109.798(7)
γ (°)	90
V (Å^3)	2308.3(19)
Z	1
Calculated density (g/cm^3)	1.517
F(000)	1082.0
Crystal size, mm	0.22 × 0.2 × 0.18
θ range for data collection (°)	1.678–27.324
Index range h, k, l	–11/11, –29/31, –14/13
Reflections collected	13812
Independent reflections (R_{int})	5139 (0.0901)
Data/restraint/parameters	5139/369/326
Goodness-of-fit on F^2	0.986
Final R_1, wR_2 [$I > 2\sigma(I)$]	R_1 = 0.0665, wR_2 = 0.1528
Largest diff. peak and hole	0.66/–0.43

Table S2. The selected bond lengths (Å) and angles (°) for **1**

Parameter	Value (Å/°)	Parameter	Value (Å/°)
Zn1–O4	2.327(2)	Zn1–O3	2.077(1)
Zn1–N3	2.046(4)	Zn1–N1	2.154(5)
Zn1–O1^{i}	2.344(2)	Zn1–O2^{i}	2.071(2)
O4–Zn1–O1^{i}	86.32(6)	O3–Zn1–O4	60.05(4)
O3–Zn1–N1	101.07(6)	O3–Zn1–O1^{i}	95.72(1)
N3–Zn1–O4	89.64(4)	N3–Zn1–O3	141.26(5)
N3–Zn1–N1	78.49(2)	N3–Zn1–O1^{i}	106.53(9)
N3–Zn1–O2^{i}	111.22(1)	N1–Zn1–O4	128.57(5)
N1–Zn1–O1^{i}	145.28(4)	O2^{i}–Zn1–O4	142.32(7)
O2^{i}–Zn1–O3	107.53(1)	O2^{i}–Zn1–N1	87.48(4)
O2^{i}–Zn1–O1^{i}	58.44(4)		

Symmetry code: ^{i} = 1/2+x, 3/2–y, –1/2+z

Table S3. Comparison of analytical methods for the detecting NOR

	Method	Sensing material	LOD	Ref.
1	Electrochemical sensor	MWCNTs	46 nmol/L	[42]
2	Electrochemiluminescence	Terbium complex	0.69 nmol/L	[43]
3	Chromatography with fluorescent	Nile Blue perchlorate	469.73 nmol/L	[44]
4	Fluorescence quenching	Sulfur quantum dot	3300 nmol/L	[45]
5	Fluorescence quenching	Metal organic framework	180 nmol/L	[46]
6	Fluorescence quenching	CP	0.159 nmol/L	This work

Table S4. The HOMO-LUMO energies calculated for selected analytes

Analytes	HOMO (eV)	LUMO (eV)	Band Gap (eV)	Ref.
CIP	−5.71	−1.18	4.53	[53]
SMX	−6.12	−1.18	4.94	[54]
SDZ	−6.25	−1.85	4.40	[45]
SMZ	−5.63	−1.82	3.81	[46]
RNZ	−6.57	−1.12	5.45	[46]
ENR	−6.26	−1.84	4.42	[46]
ORN	−7.11	−2.59	4.52	[55]
MDZ	−6.01	−2.67	3.34	[56]
LEV	−5.96	−1.71	4.25	[43]
NOR	−6.45	−2.02	4.43	[43]

Section 3. Supplementary Figures

Fig. S1. The FTIR spectra of the compound and the L ligand.

Fig. S2. View of the 1D $[Zn(mip)]_n$ chain made of metal centers and mip^{2-}.

Fig. S3. The 3-connected 2D **hcb** topological structure of **1** (cyan balls: Zn(II) centers; red sticks: bridging L ligands; blue-violet sticks: mip^{2-} ligand).

Fig. S4. Chair-like six-membered ring in **1**.

Fig. S5. PXRD patterns for **1** before and after experiments.

Fig. S6. (a) The TG curve of **1**; **(b)** The PXRD patterns of the remaining residue of **1** and the standard ZnO.

Fig. S7. The emission intensities of **1** in aqueous solution for 12 h.

Fig. S8. The emission intensities **(a)** and the PXRD patterns **(b)** of **1** after dissolving in aqueous solution with different pH values.

Fig. S9. The UV-DRS spectrum of **1**.

Fig. S10. Solid-state luminescent spectra **(a)** and the coordinates pictured in CIE chromaticity diagram **(b)** of L ligand, **1** and H_2mip at room temperature.

Fig. S11. The fluorescence double-exponential decay curve of **1** (Reference values: $\tau_1 = 840.26$; $\tau_2 = 3192.52$; $B_1 = 1427.45$; $B_2 = 276.99$, $\chi^2 = 1.020$).

Fig. S12. Emission intensities of **1** in different antibiotic aqueous solutions.

Fig. S13. The fluorescence intensity changes of the aqueous **1** suspensions containing interference substances upon the incremental addition NOR in comparison with that for a **1** suspension without any interference.

Fig. S14. (a) The luminescent intensity of **1** to detect NOR after three cycles; **(b)** The PXRD

spectra of **1** after each experiment.

Fig. S15. The emission intensities (Left) and CIE chromaticity diagram (Right) of **1** with the concentration of NOR increases.

Fig. S16. Luminescence spectra of **1** after the addition of NOR at different time.

Fig. S17. The Mott−Schottky curve of **1**.

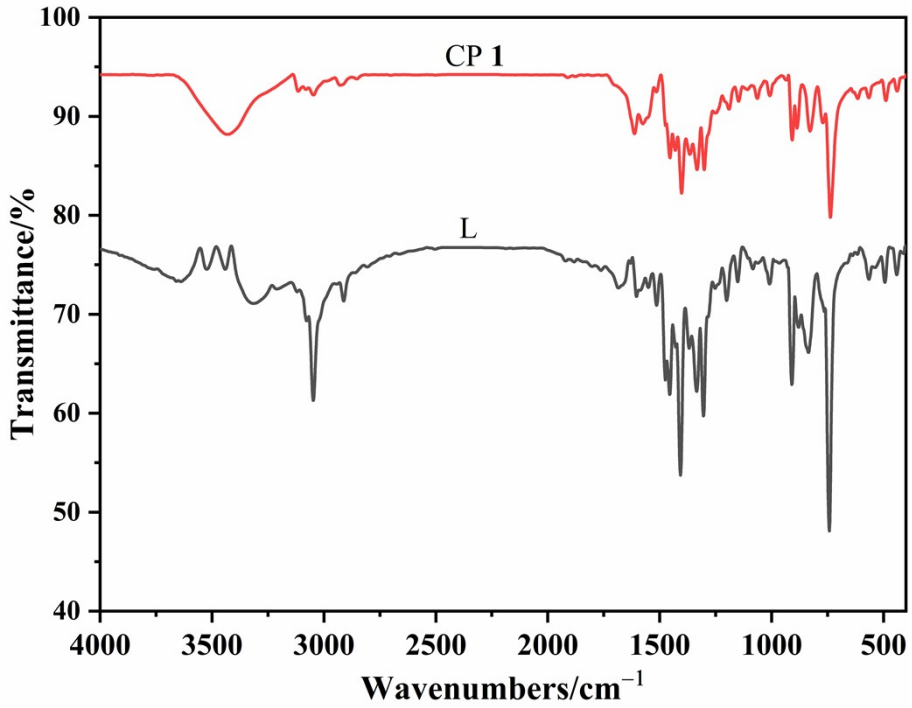

Fig. S1 The FTIR spectra of **1** and the L ligand.

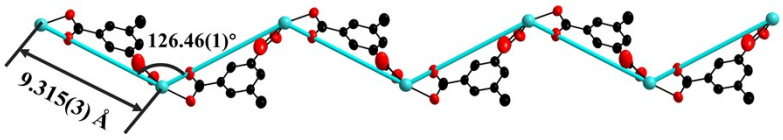

Fig. S2. View of the 1D $[Zn(mip)]_n$ chain made of metal centers and mip^{2-}.

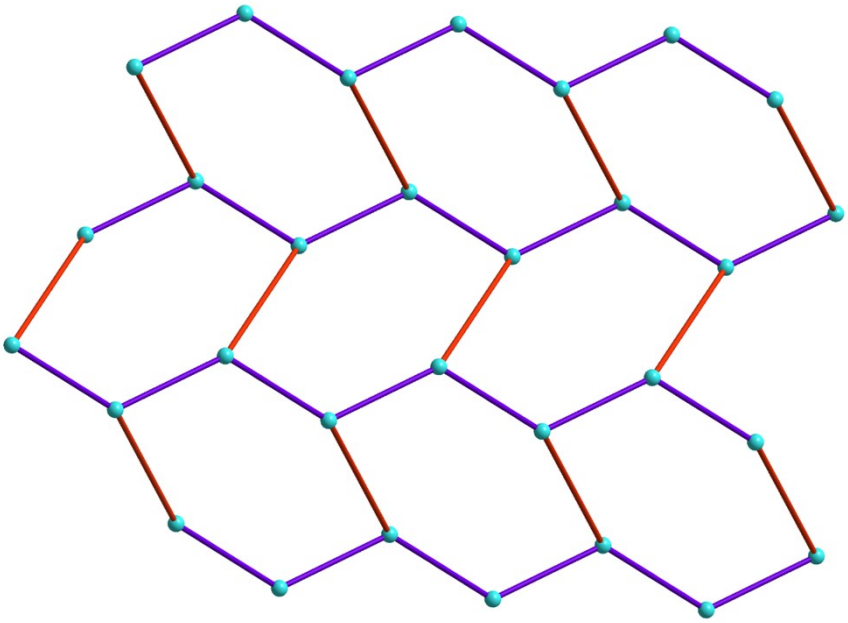

Fig. S3. The 3-connected 2D **hcb** topological structure of **1** (cyan balls: Zn(II) centers; red sticks: bridging L ligands; blue-violet sticks: mip^{2-} ligand).

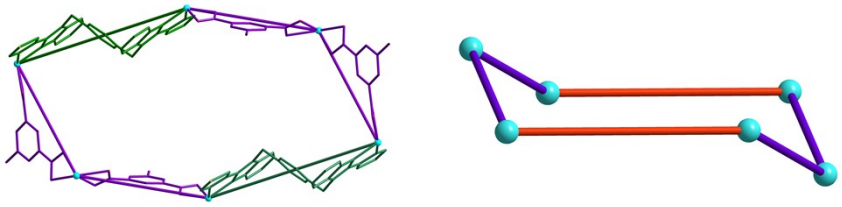

Fig. S4. Chair-like six-membered ring in **1**.

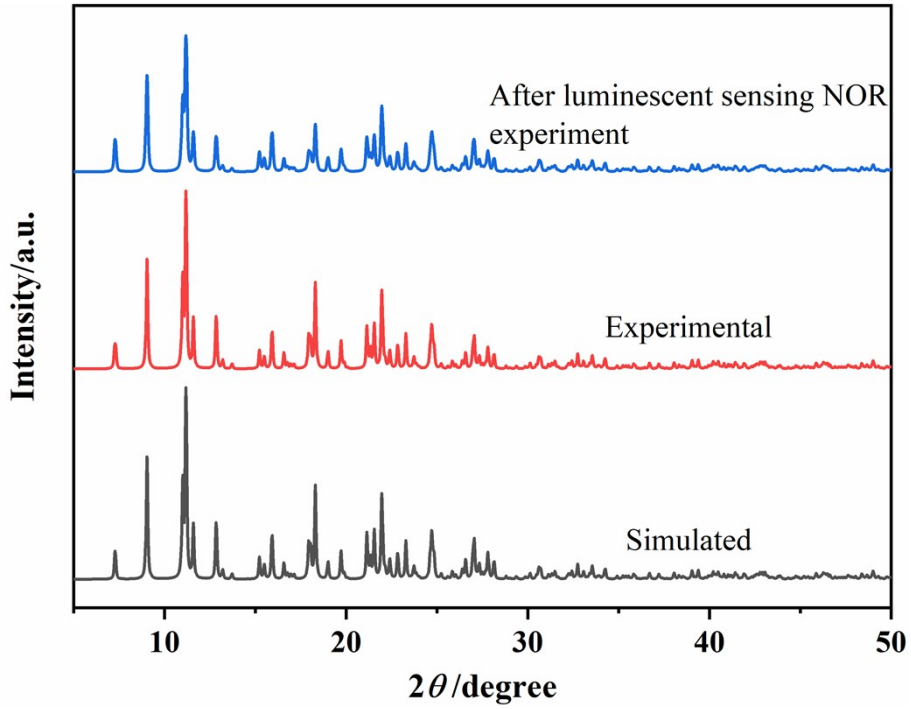

Fig. S5. PXRD patterns for **1** before and after experiments.

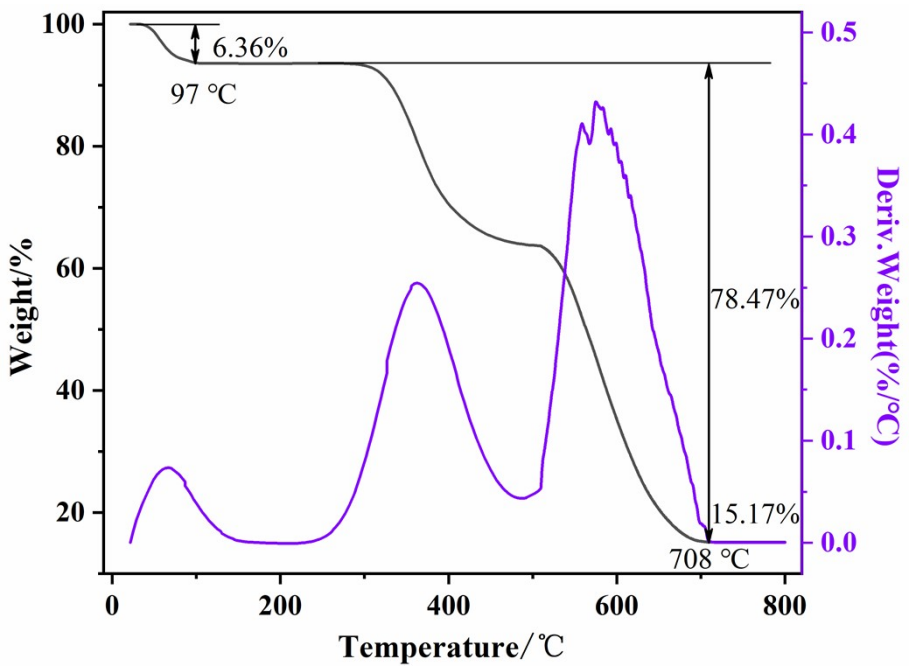

(a)

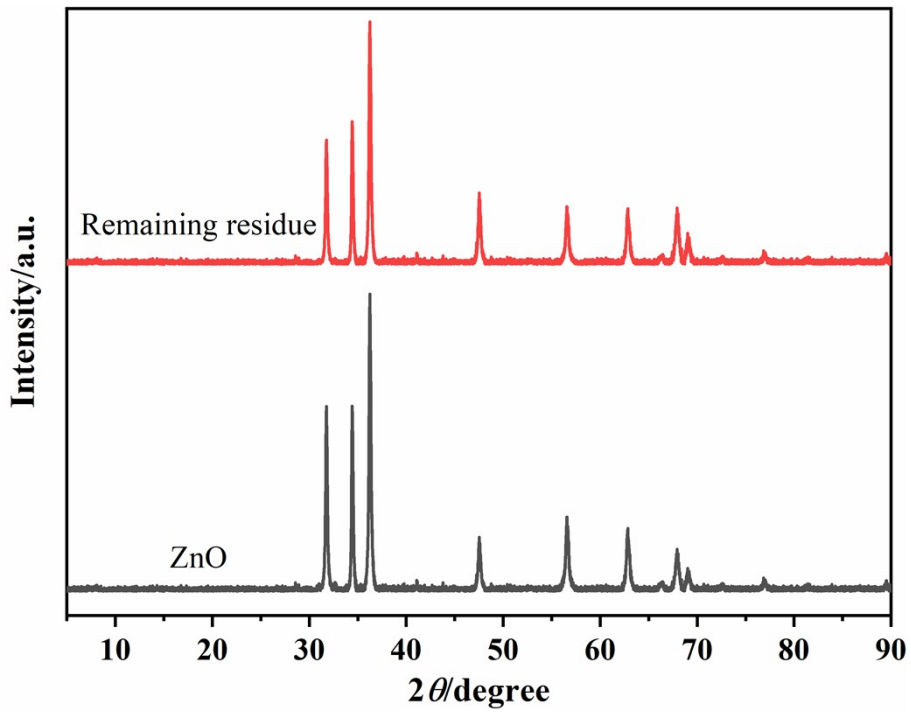

(b)

Fig. S6. (a) The TG curve of **1**; **(b)** The PXRD patterns of the remaining residue of **1** and the standard ZnO.

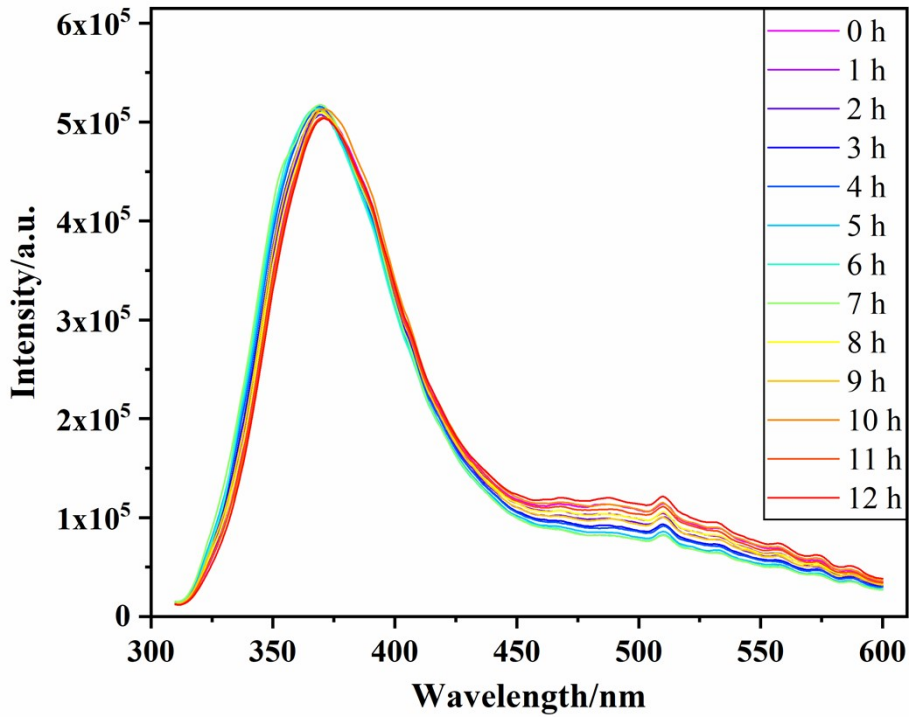

Fig. S7. The emission intensities of **1** in aqueous solution for 12 h.

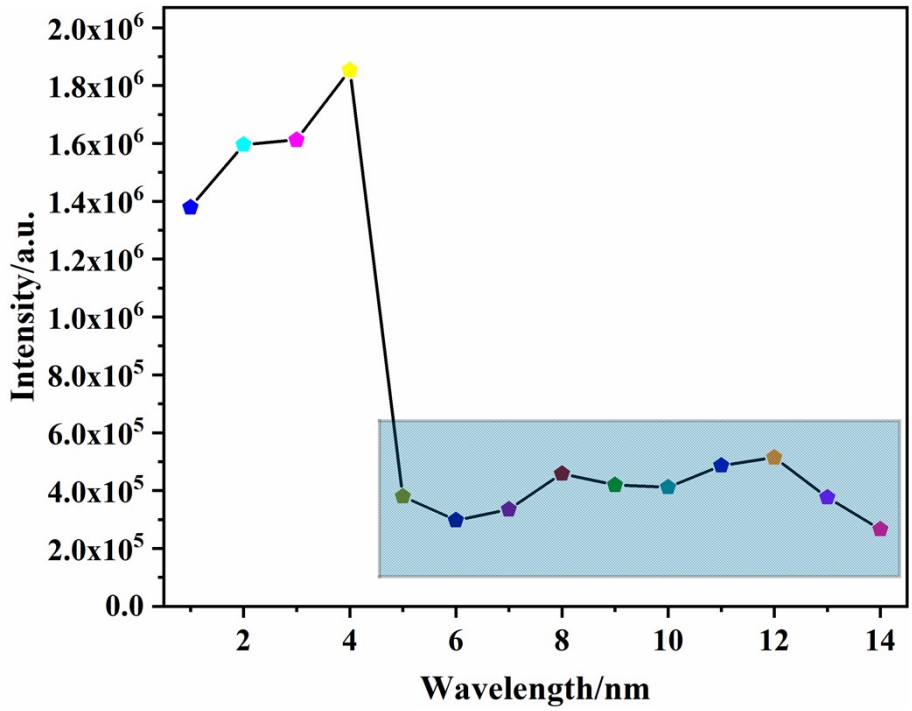

(a)

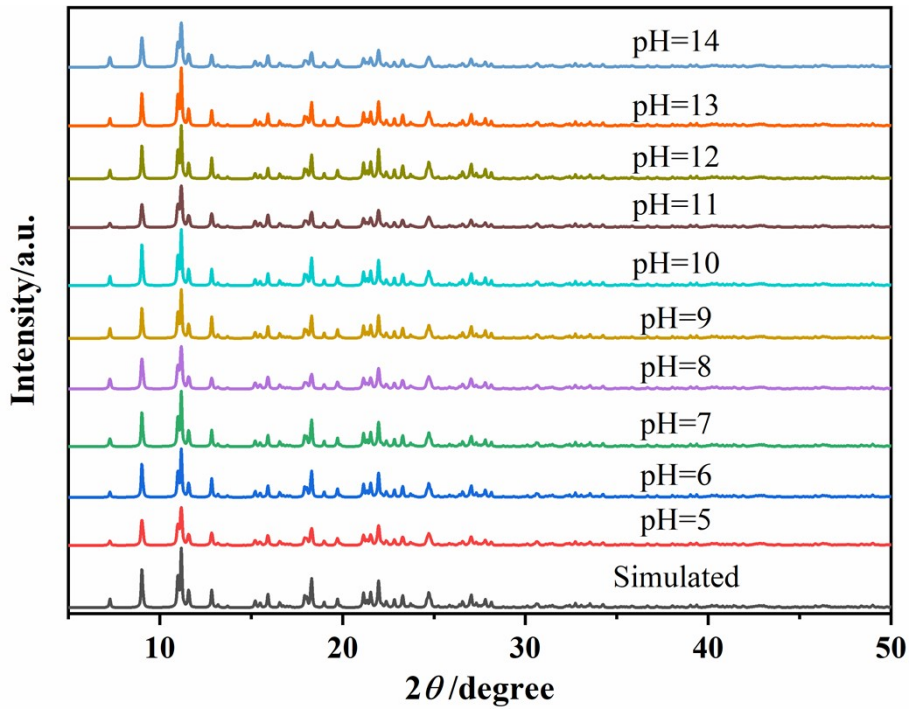

(b)

Fig. S8. The emission intensities **(a)** and the PXRD patterns **(b)** of **1** after dissolving in aqueous solution with different pH values.

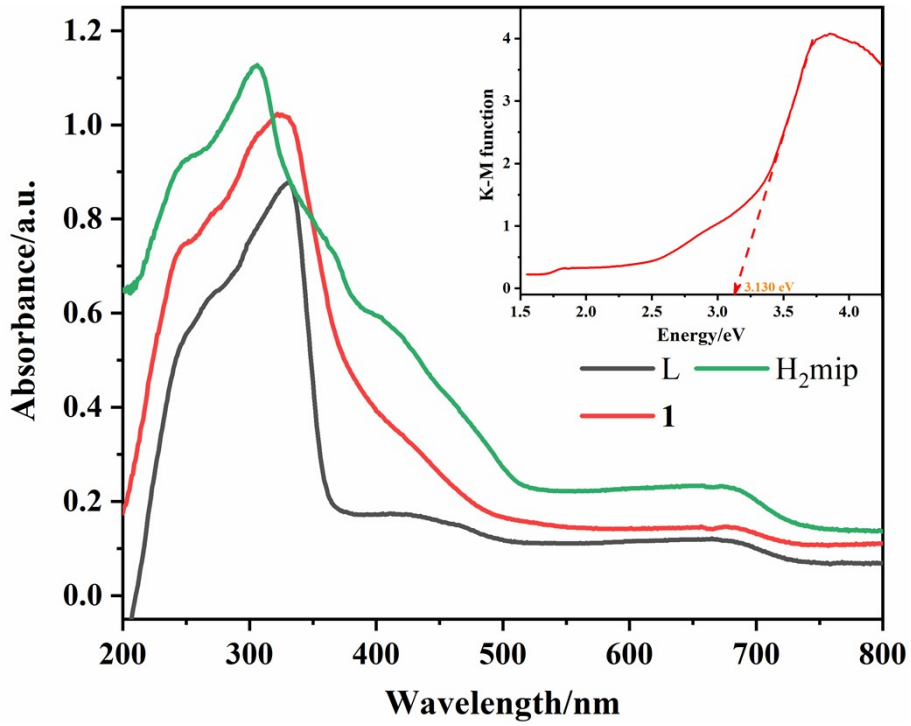

Fig. S9. The UV-DRS spectrum of **1**.

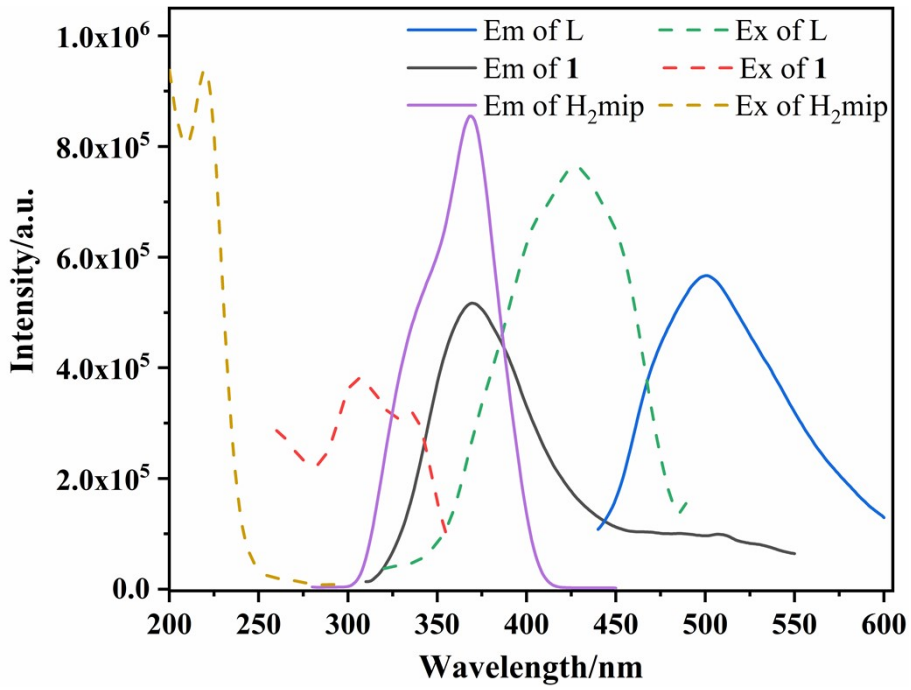

(a)

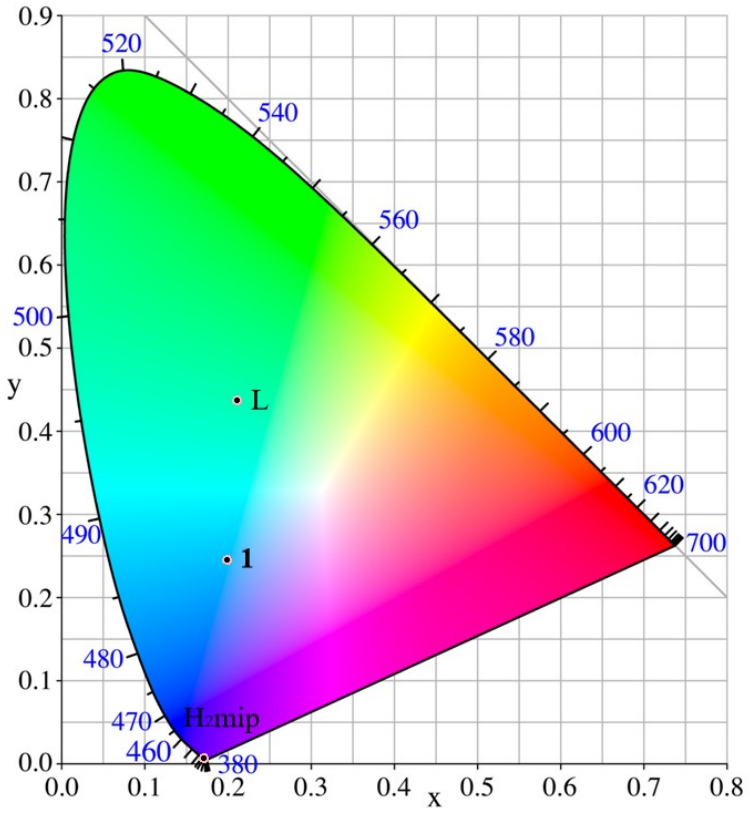

(b)

Fig. S10. Solid-state luminescent spectra **(a)** and the coordinates pictured in CIE chromaticity diagram **(b)** of L ligand, **1** and H_2mip at room temperature.

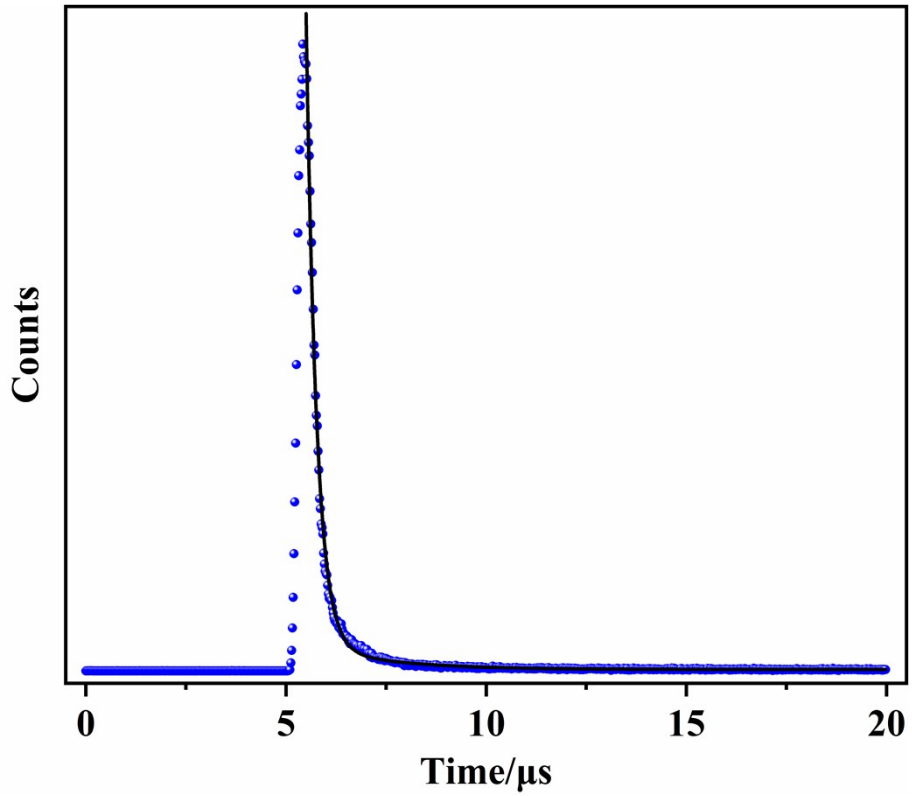

Fig. S11. The fluorescence double-exponential decay curve of **1** (Reference values: τ_1 = 840.26; τ_2 = 3192.52; B_1 = 1427.45; B_2 = 276.99, χ^2 = 1.020).

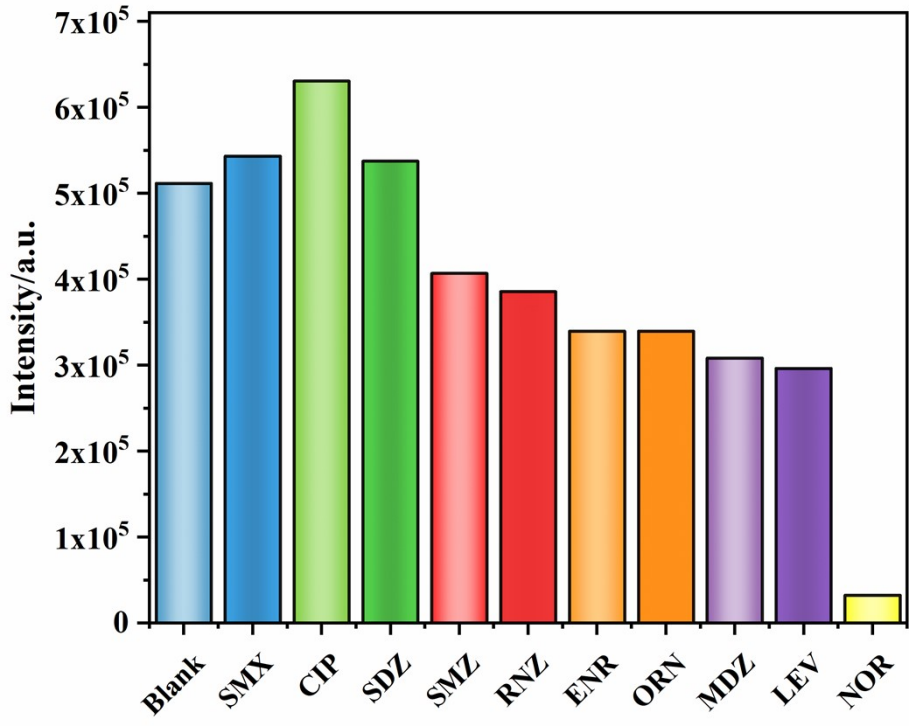

Fig. S12. Emission intensities of **1** in different antibiotic aqueous solutions.

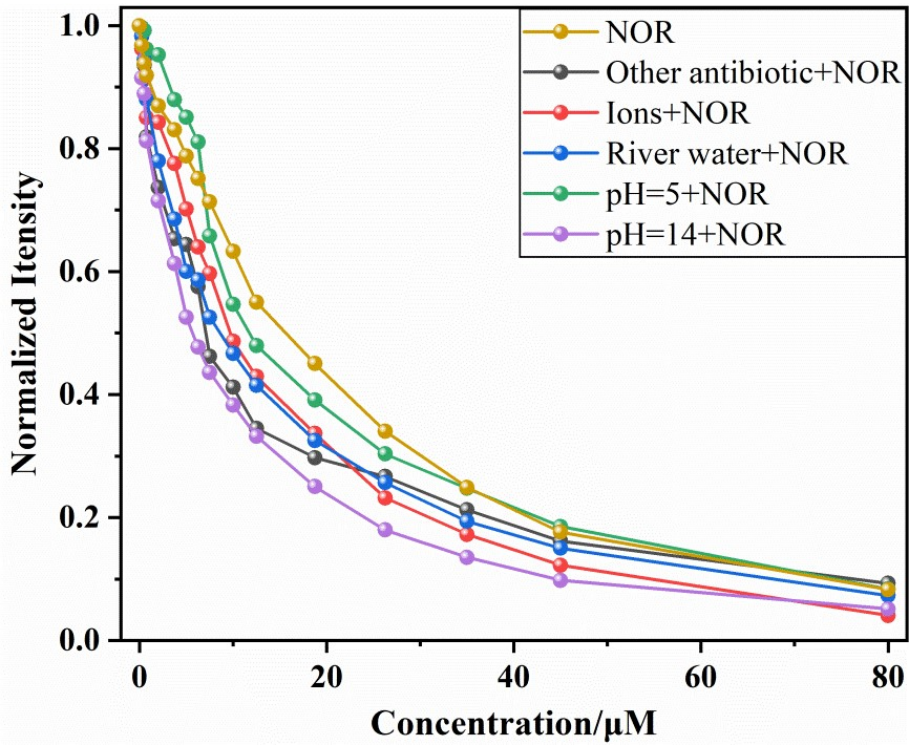

Fig. S13. The fluorescence intensity changes of the aqueous **1** suspensions containing interference substances upon the incremental addition NOR in comparison with that for a **1** suspension without any interference.

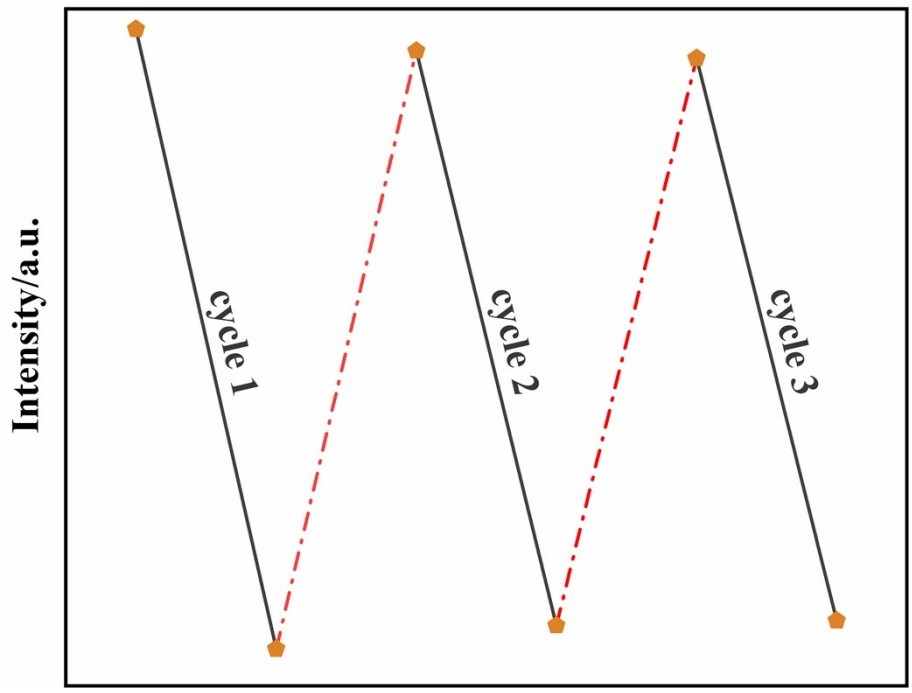

(a)

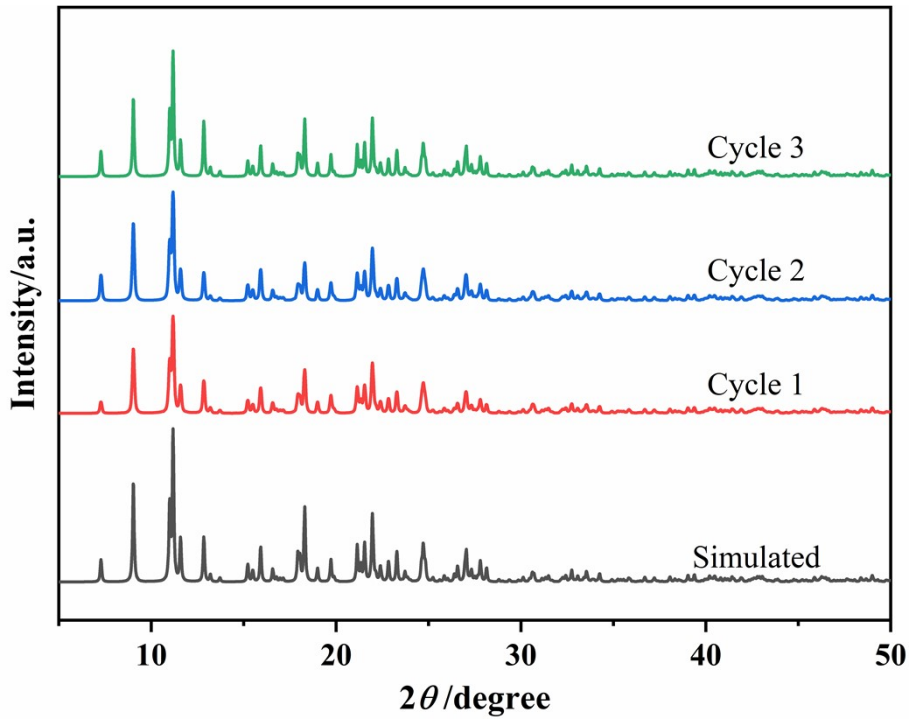

(b)

Fig. S14. (a) The luminescent intensity of **1** to detect NOR after three cycles; **(b)** The PXRD spectra of **1** after each experiment.

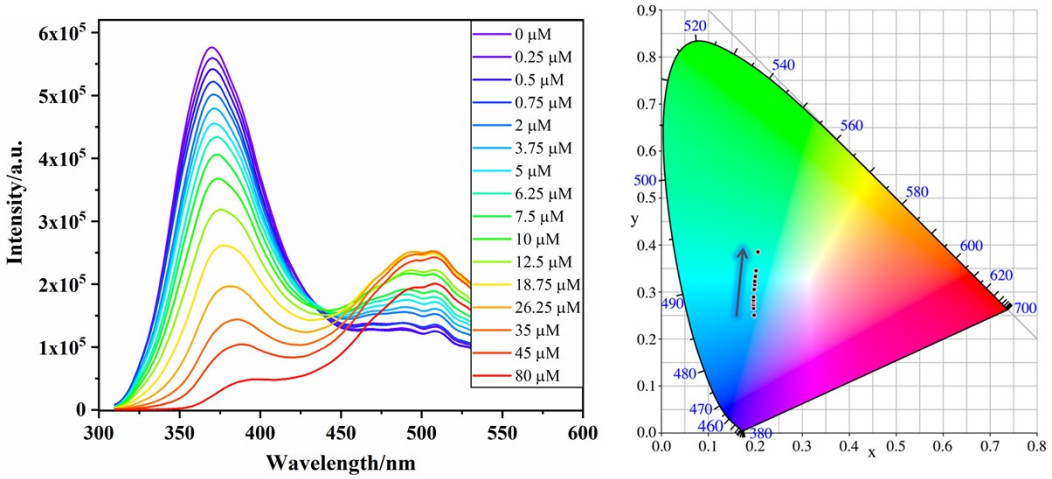

Fig. S15. The emission intensities (Left) and CIE chromaticity diagram (Right) of **1** with the concentration of NOR increases.

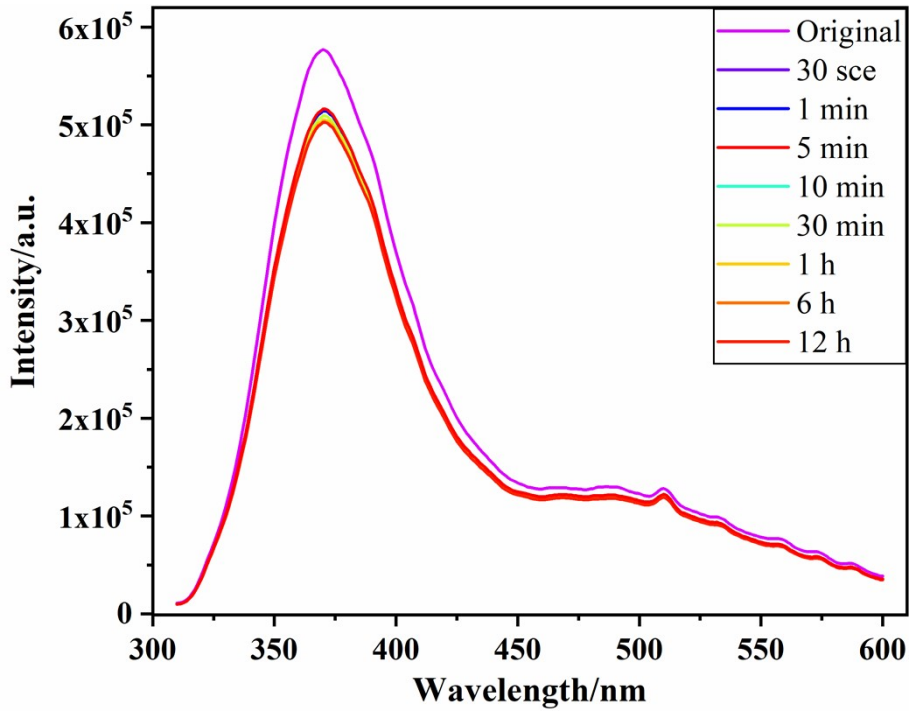

Fig. S16. Luminescence spectra of **1** after the addition of NOR at different time.

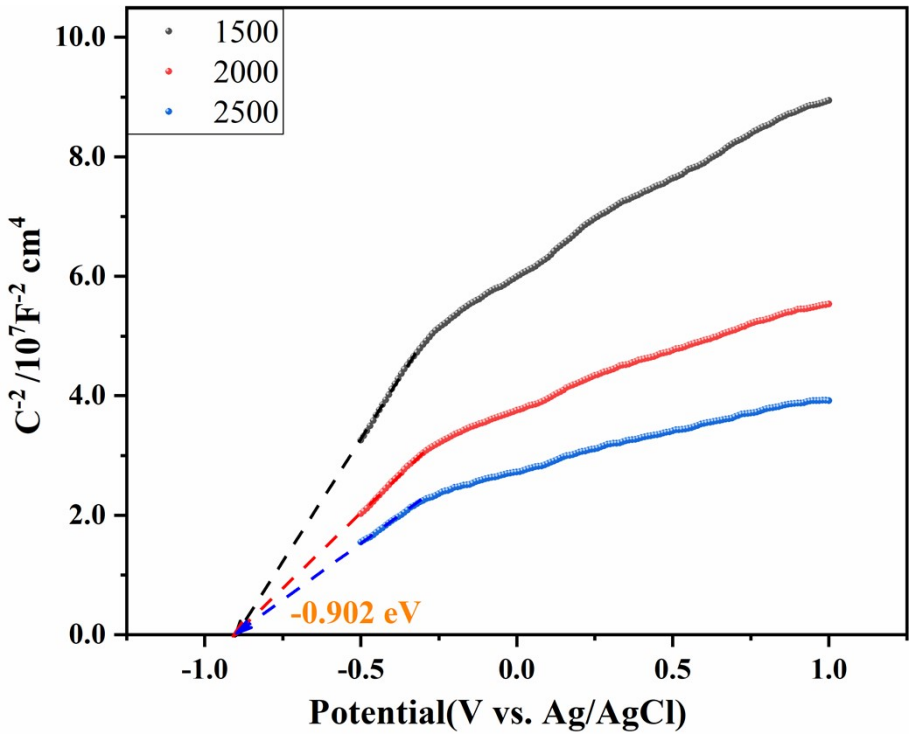

Fig. S17. The Mott−Schottky curve of **1**.